



UNIVERSITEIT•STELLENBOSCH•UNIVERSITY  
jou kennisvenoot • your knowledge partner

*Mass and volume optimization of a permanent magnet vernier machine  
(repository copy)*

---

**Article:**

Tlali, P.M., Wang, R-J., (2017) Mass and volume optimization of a permanent magnet vernier machine, *Proc. of the 25th Southern African Universities Power Engineering Conference, (SAUPEC)*, pp. 315--319, Stellenbosch, 30 Jan. - 1 Feb. 2017.

---

**Reuse**

Unless indicated otherwise, full text items are protected by copyright with all rights reserved. Archived content may only be used for academic research.

# MASS AND VOLUME OPTIMIZATION OF A PERMANENT MAGNET VERNIER MACHINE

P.M. Tlali\* and R-J. Wang\*

\* Department of Electrical & Electronic Engineering, Stellenbosch University, Private Bag XI, Matieland 7602, South Africa, E-mail: 15894215@sun.ac.za; rwang@sun.ac.za

**Abstract:** In this paper, the finite element analysis (FEA) based design optimization of a surface-mounted permanent magnet (PM) vernier machine is presented. The rapidly increasing weight and size of the machine is usually one of the major concerns in low operating speed directly driven wind turbine configurations. Hence, the total mass and volume are chosen as the main optimization objectives for the current study, and these are investigated at various pole/slot combinations and machine aspect ratios. Moreover, core loss and torque behavior of the optimized machines are also presented since those are some of the performance indexes directly related to the pole/slot combination. The obtained results show that in PMV machines, it is feasible to realize a compact design with fairly good torque quality.

**Key words:** vernier machines, permanent magnet, magnetic gearing effects, finite element analysis, design optimization.

## 1. INTRODUCTION

With the steady growth of the global demand for wind energy, the dimensional size and output capacity of wind turbines have also been increasing over years [1]. This development has simultaneously translated into manufacturing of large generators that can handle large torques and convert most of the power captured by the turbine blades. But the challenge is that both the volumetric size and weight of the generator have maximum limits imposed by, among other factors, the cost and the fact that it has to be elevated onto the tower. Currently, the most popular way of approaching this generator size issues is by implementing a cascaded connection of a gearbox and medium/high speed generator, called a geared system. However, this arrangement is also not a perfect solution under certain application conditions such as in offshore locations due to its reliability concerns. Thus, directly driven generators (DDGs) remain possible options despite their known heavy weights and large sizes in comparison to the geared systems. For power electronic converter (PEC) interfaced grid connection, permanent magnet synchronous machines (PMSM) are arguably the most promising type of DDGs because of their better efficiency and relatively good torque density [2,3].

In the past decade, the permanent magnet vernier (PMV) machine has emerged as an attractive alternative to either DDGs or geared systems. By virtue of the magnetic gearing principle inherent in them, PMV machines render superior torque density than PMSM while they also have similar structural simplicity [4,5]. This feature obviously gives an impression that, at the same output power or torque rating, a PMV machine would be lighter and more compact relative to the PMSM. There has been some comparative studies previously made between these two machines types [6–8]. Most of the aforementioned studies followed a traditional method of comparison whereby the

output power or torque density is optimized within a fixed machine volume. In other words, the motor torque is maximized through variation of the internal dimensions. This is logical in the cases where the physical dimensions are constrained by the available space of target application. But for the purpose of performance comparison or if no space limitations given, it is reasonable to let the outer motor dimensions vary since many other parameters depend on them.

This paper aims at optimizing the mass and volume of the PMV machine for the same rated output power and torque. In addition, a traditional synchronous PM machine is included as a benchmark to the range of considered machines. Consequently, it will then be clear if any significant advantages regarding the mentioned aspects are to be obtained from PMV relative to PMSM. The optimization is done for a few combinations of pole/slot numbers so that the effect of gear ratio is also included in the study. Furthermore, the aspect ratio is optimized to allow the machines to be designed at their best shape. Lastly, the machines' torque behavior and core losses at optimized dimensional parameters are also presented.

## 2. SELECTION OF POLE-SLOT COMBINATIONS

The cross-sectional view of a conventional three-phase PMV machine investigated in this paper is shown in Fig. 1. Both the rotor yoke and the stator core are constructed by the steel lamination. Moreover, the rotor has many surface-mounted permanent-magnets with alternating polarity, while the stator slots host a common distributed 3-phase winding. Although its structure may largely look like that of the conventional PMSM, the difference is that the numbers of stator and rotor pole-pairs are always in-equivalent to each other. Hence the stator teeth number have to be chosen in such a way that, in addition to being the flux path, they will also act to

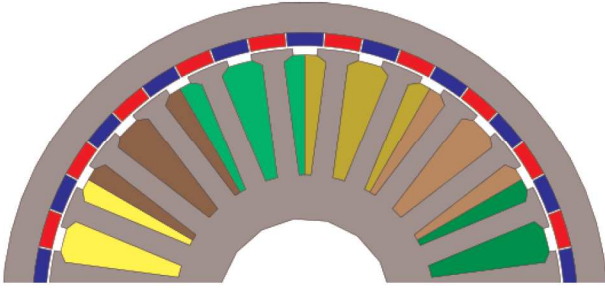


Figure 1: Conventional PM vernier machine.

modulate the magnetic fields from the rotor PMs.

Equation 1 is regarded as the deterministic relationship between the valid number of flux modulating pieces and the rotor and/or stator pole-pairs according to the flux modulation principle.

$$N_s = p_r \pm p_s \quad (1)$$

where  $N_s$ ,  $p_r$  and  $p_s$  are the number of flux modulating pieces, rotor PM pole-pairs and stator pole-pairs respectively. For a conventional PM Vernier machine, the number of modulating pieces actually correspond to that of stator teeth, which means their number and that of the stator pole-pairs must also abide by the rules stipulated in normal synchronous PM machine design, the most prominent one in the three-phase machine being that:

$$\frac{Q}{\text{GCD}(Q, p_s)} = 3k, \quad k = 1, 2, 3, \dots \quad (2)$$

where GCD means the greatest common denominator and Q is the stator slot number.

The speed or torque gearing ratio  $G_r$  is defined as the ratio between the rotor and stator pole-pair numbers. Correspondingly, a larger difference between  $p_r$  and  $p_s$  gives a higher  $G_r$ , and in the case that  $G_r$  is equal to unity, then the machine can be referred to as the conventional synchronous PM machine instead.

$$G_r = -|2pq - 1| = -\frac{p_r}{p_s} \quad (3)$$

$$q = \frac{Q}{2p_s m} \quad (\text{m: number of phases})$$

For a given machine diameter, the upper limit to  $p_r$  is usually imposed by the PM inter-polar leakage flux that becomes more prevalent in large  $p_r$  numbers. Generally, the suitable  $G_r$  is chosen on the basis of the intended or required speed amplification while also taking into consideration the torque ripple characteristics of each  $p_r/p_s$  combination. It has been reported that cogging or ripple torque effects are minimized by choosing fractional  $G_r$ , at the expense of lower stall torque [9]. Basically, the implication of all the above points is that the PMV machine's pole/slot combination is naturally dependent on several factors. However, in the foregoing study, the range of  $G_r$  and/or pole-slot combination was limited

Table 1: Investigated pole-slot combinations.

| Q  | $p_s$ | $G_r$ | $q$   | Freq |
|----|-------|-------|-------|------|
| 24 | 2     | 11    | 2.0   | 55.0 |
| 21 | 2     | 9.5   | 1.75  | 47.5 |
| 27 | 3     | 8.0   | 1.5   | 60.0 |
| 27 | 4     | 5.75  | 1.125 | 57.5 |
| 24 | 4     | 5.0   | 1.0   | 50.0 |
| 27 | 17    | 1.0   | 0.265 | 42.5 |

Indicated frequency is at speed of 150rpm.

The combination 27/17 is a PMSM

by the presumed machine output frequency that is to be utmost 60Hz at a rated speed of 150rpm, to minimize the frequency dependent losses. Thus, a number of investigated stator pole-slot combinations satisfying this condition are listed in Table 1. Then the total machine mass at each  $G_r$  value and constant output power (due to fixed speed, torque is also fixed) was optimized to select the best  $G_r$ . This was further carried out at various different machine aspect ratios to avoid the effect of fixing the machine diameter on flux leakage, by giving the freedom on the available PM pitch length.

### 3. DESIGN OPTIMIZATION

The objective of the overall optimization process was to minimize the machines' volume and total active mass for a fixed output power for different pole-slot combinations and aspect ratios. This was achieved by employing the gradient based modified method of feasible directions (MMFD) in VisualDOC optimization suite to solve the constrained problem formulated as [10]:

$$\begin{aligned} \text{Minimize: } & F(\mathbf{X}) = \mathbf{Y} \\ \text{Subject to: } & \eta \geq 85\% \\ & J \leq 4 \text{ A/mm}^2 \end{aligned}$$

where  $\mathbf{X}$  represents the vector of geometric variables in Fig. 2 with angle ratios defined in Eq.4, and  $\mathbf{Y}$  is a set of objectives as described below.

$$\mathbf{Y} = \begin{bmatrix} \text{Mass (M}_{\text{Total}}) \\ \text{Volume (Vol}_{\text{Total}}) \end{bmatrix}$$

$$\begin{aligned} \theta_{pm-p} &= \frac{\pi}{p_r}; & \theta_{sp} &= \frac{2\pi}{Q} \\ \sigma_{pm} &= \frac{\theta_{pm-s}}{\theta_{pm-p}}; & \sigma_s &= \frac{\theta_s}{\theta_{sp}}; & \sigma_{so} &= \frac{\theta_{so}}{\theta_s} \end{aligned} \quad (4)$$

All the machines are intended to operate under the natural air-cooling conditions, consequently, current density (J) is limited to 4 A/mm<sup>2</sup>. Due to the fact that overlapping windings were used, the slot-filling factor was also fixed at 0.4, which is practically fair considering the challenges met in such winding type manufacturing. The main parameters that define the objective search space for each considered machine are provided in Table 2 below.

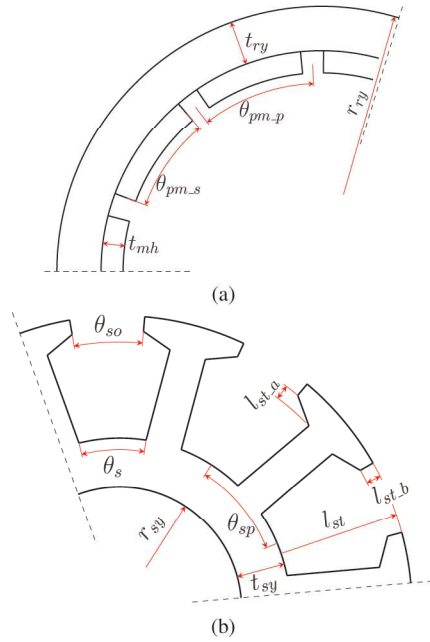


Figure 2: Machine geometric optimization variables: (a) Rotor (b) Stator.

Table 2: Main specifications for the optimized machines.

| Parameter                      | Value      |
|--------------------------------|------------|
| Output power (kW)              | 2          |
| Air-gap length (mm)            | 0.8        |
| Slot-fill factor               | 0.4        |
| Operating speed (rpm)          | 150        |
| Aspect ratio ( $\frac{L}{D}$ ) | 0.05 - 0.7 |

L = active stack length, D = total diameter.

During the optimization process, core-losses, end-winding length, end-winding's inductance and resistances were calculated using analytical equations so that their effect can be included in the performance evaluation deduced from 2D FEA static solutions. Thus, both the efficiency and power factor calculations have included the effect of end-windings. Further multi-step FEA simulations were done on the optimized machines to verify and compare their core-losses and torque characteristics.

#### 4. OPTIMIZATION RESULTS

The obtained results are given in Figs. 3 and 4, whereby it can be clearly seen that increasing the gearing ratio enables the machine to have a lower mass. This tendency is also reflected on the total volume, that with larger  $G_r$ , the machine becomes smaller. Coincidentally, it is also in good agreement with the general knowledge from a cascaded arrangement of mechanical gear-box and conventional PM synchronous machine, that the machine's mass and volume will both be minimized. In contrast, the PMV machine's power factor (PF) decreases with increasing  $G_r$  as indicated in Table 3, which is to be expected since it's torque is known to be inversely

proportional to the PF. This means one can not just choose a high  $G_r$  value to fulfill the required torque, but the PF has to be taken into consideration since it directly relates to the size of the converter to be used.

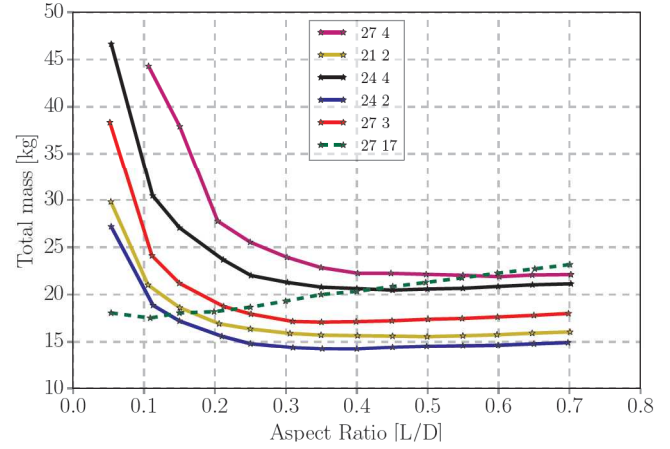


Figure 3: Machine mass vs aspect ratio.

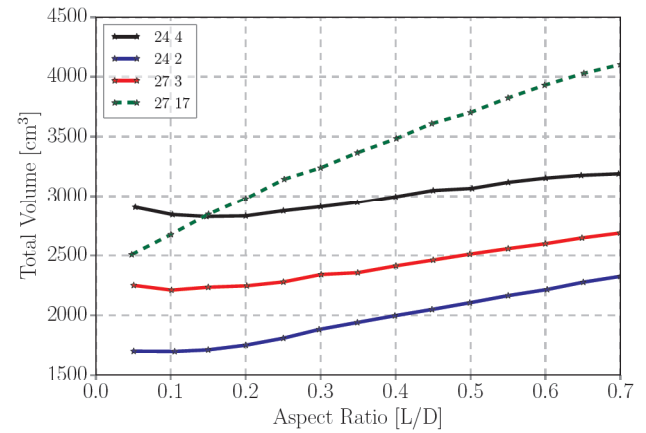


Figure 4: Machine volume vs aspect ratio.

Table 3: Mass and average power factors for different pole-slot combinations.

| Q  | $p_s$ | $G_r$ | PF   | Mass [kg] |
|----|-------|-------|------|-----------|
| 24 | 2     | 11    | 0.63 | 14.4      |
| 21 | 2     | 9.5   | 0.69 | 15.96     |
| 27 | 3     | 8.0   | 0.77 | 17.28     |
| 27 | 4     | 5.75  | 0.86 | 23.67     |
| 24 | 4     | 5.0   | 0.89 | 21.25     |
| 27 | 17    | 1.0   | 0.95 | 19.23     |

A general machine sizing approach for both the PMV and PMSM, uses the  $D^2L$  product equation (Eq. 5) which approximates the torque or output power based on the stator volume, given the magnetic and electrical loading [11].

$$D^2L = \frac{4P}{\pi\omega_m\eta k_\omega \hat{B}_g \hat{K}_s} \quad (5)$$

where P is the output power,  $\hat{B}_g$  and  $\hat{K}_s$  are the air-gap flux



density and stator electric loading, respectively, and  $k_{\omega}$  is the armature winding factor.

Thus, the diameter and stack length are also some parameters to investigate, and this is normally done using the term commonly known as 'Aspect ratio' defined as  $L/D$ . As can be read from Fig. 3, the PMVs' machine weight is significantly high at very low aspect ratios, but this tends to decrease with increasing  $L/D$  values up to a certain point after which no change could be seen. On the other hand, the trend of results is completely different for the volume (Fig. 4) as it constantly increase with aspect ratio. For the PMSM, both the mass and volume increase proportionally to the aspect ratio. Therefore, with reference to the presented results, an aspect ratio of 0.3 was chosen because it seems to be a good trade-off in terms of the lowest mass and moderate volume.

## 5. TORQUE CHARACTERISTICS AND CORE LOSSES

In PM excited and iron cored slotted machines, cogging and torque ripples are naturally caused by the PM interaction with the stator teeth. Consequently, a good indication to the percentage magnitude of these performance index is derived by examining the lowest common multiple (LCM) between the PM pole-pair and stator teeth numbers. A higher LCM value is more favourable as it predicts less cogging or ripple percentage. In this study, the torque characteristics were calculated using the multi-step static FEA, with the machines' dimensions fixed for an aspect ratio of 0.3. The obtained waveforms for cogging torque are shown in Fig. 5 and for torque ripple shown in Fig. 6. These results are further summarized in Table 4. Most of the obtained cogging or torque ripples are less than 5%, which is practically acceptable for most applications. Also, it is interesting to note that, even though the PMSM (27/17) has very large LCM, its torque ripple is one of the worst. Hence, it can be seen that PMV machines are generally smooth torque machines.

Table 4: Torque characteristics of different pole/slot combinations.

| Pole/slot comb. | LCM | Ave.Torque [Nm] | Torque ripple[%] | Cogging torque[%] |
|-----------------|-----|-----------------|------------------|-------------------|
| 24/2            | 24  | 142.73          | 2.73             | 2.81              |
| 21/2            | 42  | 144.74          | 1.21             | 0.95              |
| 27/3            | 27  | 146.05          | 1.58             | 0.68              |
| 27/4            | 108 | 144.44          | 2.78             | 0.28              |
| 24/4            | 24  | 150             | 13.40            | 12.84             |
| 27/17           | 459 | 142.53          | 4.55             | 2.61              |

Core losses are a function of flux density magnitude, volume of iron material within a machine and mainly the rate of change of flux density. Thus, at any given input speed, pole/slot combinations with a higher frequency are likely to have higher losses than others. Again, using the same multi-step static FEA as in torque analysis, the

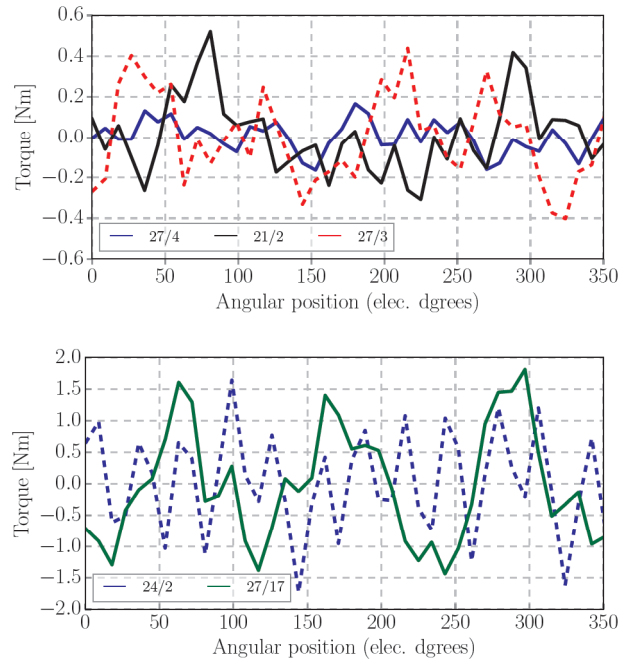


Figure 5: Cogging torque.

core losses are approximated using the Steinmetz based equation (Eq. 6) [12, 13]. Since this model equation uses flux variation and magnitude deduced from several independent static solutions, it gives satisfactory accuracy albeit much faster compared to transient FEM simulations.

$$P_{core} = \frac{1}{T} \int_0^T C_{SE} \left| \frac{dB}{dt} \right|^\alpha |\Delta B|^{\beta-\alpha} dt \quad (6)$$

where  $T$  is the period,  $\Delta B$  is the peak-to-peak flux density,  $C_{SE}$ ,  $\alpha$  and  $\beta$  are the lamination material loss model coefficients.

The calculated core losses at different speeds are plotted in Fig. 7. It can be clearly seen that due to the lower frequency, the PMSM has considerably lowest losses and the PMV pole/slot combination with highest frequency (27/3) is the worst. The other PMV machine's slot combinations fall in the middle range depending on their iron mass and frequency.

## 6. CONCLUSIONS

The mass and volume of a PM vernier machine have been investigated in this paper. It has been shown that they can both be minimized by selecting a pole/slot combination with a higher gear ratio. This is a clear advantage over a PM synchronous machine which is considered to be limited only to a unity gear ratio, since the PMV can be designed to be lighter and smaller for the same output power. However, it is also important to note that while larger gear ratio allows compact PMV design, the power factor gets extremely low, which results into a bigger sized converter requirement. The aspect ratio was observed to have a notable influence on the mass and total volume

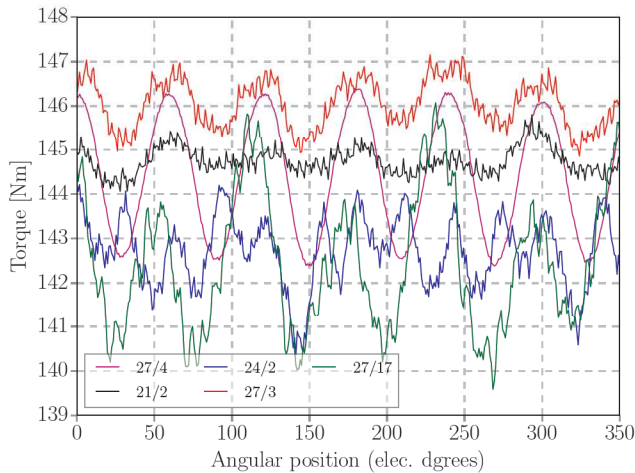


Figure 6: Torque ripple.

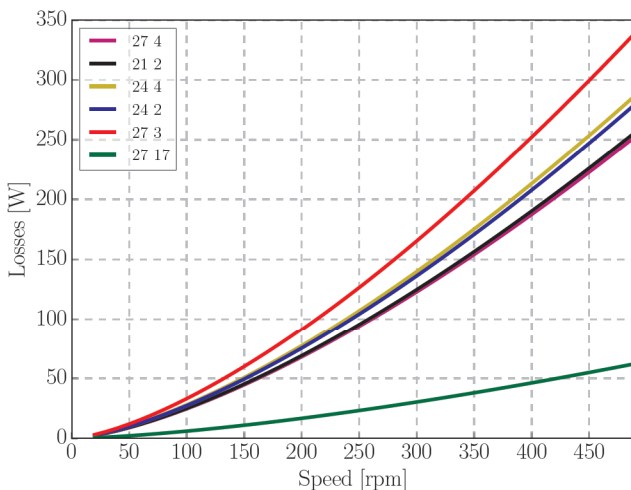


Figure 7: Core losses as a function of speed.

as well. Furthermore, the torque characteristics of the PMV machine are also found to have comparatively good quality.

#### ACKNOWLEDGMENT

This work was supported by ABB Corporate Research, Sweden.

#### REFERENCES

[1] G. Shrestha, H. Polinder and J.A. Ferreira, "Scaling laws for direct drive generators in wind turbines," *Electric Machines and Drives Conference. IEMDC '09. IEEE International*, Miami, FL, 2009, pp. 797-803.

[2] H. Polinder, F.F.A. van der Pijl, G.J. de Vilder and P. Tavner, "Comparison of direct-drive and geared generator concepts for wind turbines," *IEEE International Conference on Electric Machines and Drives*, 2005, San Antonio, TX, pp. 543-550.

[3] H. Li and Z. Chen, "Overview of different wind generator systems and their comparisons," in *IET Renewable Power Generation*, vol. 2, no. 2, pp. 123-138, June 2008.

[4] B. Kim and T.A. Lipo, "Operation and design principles of a PM vernier motor," *IEEE Transactions on Industry Applications*, vol. 50, no. 6, pp. 3656-3663, Nov.-Dec. 2014.

[5] J. Li and K.T. Chau, "Performance and cost comparison of permanent-magnet vernier machines," *IEEE Transactions on Applied Superconductivity*, vol. 22, no. 3, pp. 5202304, June 2012.

[6] W.N. Fu and S.L. Ho, "A quantitative comparative analysis of a novel flux-modulated permanent-magnet motor for low-speed drive," *IEEE Transactions on Magnetics*, vol. 46, no. 1, pp. 127-134, Jan. 2010.

[7] C. Liu, C.H.T. Lee and M. Chen, "Comparison of outer-rotor permanent magnet machines for in-wheel drives," *Industrial Electronics (ISIE), 2013 IEEE International Symposium on*, Taipei, Taiwan, pp. 1-6.

[8] S. Gerber and R-J. Wang, "Design and evaluation of a PM vernier machine," *2015 IEEE Energy Conversion Congress and Exposition (ECCE)*, Montreal, QC, pp. 5188-5194.

[9] N.W. Frank and H.A. Toliyat, "Gearing ratios of a magnetic gear for wind turbines," *IEEE International Electric Machines and Drives Conference*, Miami, FL, 2009, pp. 1224-1230.

[10] Vanderplaats Research & Development, Inc., Colorado Springs, CO, USA. *VisualDOC Users Manual*, Version 7, 2013.

[11] Y. Fan, L. Zhang, J. Huang and X. Han, "Design, analysis, and sensorless control of a self-decelerating permanent-magnet in-wheel motor," *IEEE Transactions on Industrial Electronics*, vol. 61, no. 10, pp. 5788-5797, Oct. 2014.

[12] A. Krings, S. Nategh, A. Stening, H. Grop, O. Wallmark, and J. Soulard, "Measurement and modeling of iron losses in electrical machines," in *Proceedings of the 5th International Conference Magnetism and Metallurgy*, Gent, Belgium, Jun. 2012, pp. 101-119.

[13] Jieli Li, T. Abdallah and C.R. Sullivan, "Improved calculation of core loss with nonsinusoidal waveforms," *Industry Applications Conference*, 2001. Thirty-Sixth IAS Annual Meeting. Conference Record of the 2001 IEEE, Chicago, IL, USA, vol. 4, pp. 2203-2210.